



This is a repository copy of *Self-Learning MTPA Control of Interior Permanent-Magnet Synchronous Machine Drives Based on Virtual Signal Injection*.

White Rose Research Online URL for this paper:  
<http://eprints.whiterose.ac.uk/105457/>

Version: Accepted Version

---

**Article:**

Sun, T. [orcid.org/0000-0002-5518-0315](http://orcid.org/0000-0002-5518-0315), Wang, J. [orcid.org/0000-0003-4870-3744](http://orcid.org/0000-0003-4870-3744), Koc, M. [orcid.org/0000-0003-1465-1878](http://orcid.org/0000-0003-1465-1878) et al. (1 more author) (2016) Self-Learning MTPA Control of Interior Permanent-Magnet Synchronous Machine Drives Based on Virtual Signal Injection. *IEEE Transactions on Industry Applications*, 52 (4). pp. 3062-3070. ISSN 0093-9994

<https://doi.org/10.1109/TIA.2016.2533601>

---

**Reuse**

Unless indicated otherwise, fulltext items are protected by copyright with all rights reserved. The copyright exception in section 29 of the Copyright, Designs and Patents Act 1988 allows the making of a single copy solely for the purpose of non-commercial research or private study within the limits of fair dealing. The publisher or other rights-holder may allow further reproduction and re-use of this version - refer to the White Rose Research Online record for this item. Where records identify the publisher as the copyright holder, users can verify any specific terms of use on the publisher's website.

**Takedown**

If you consider content in White Rose Research Online to be in breach of UK law, please notify us by emailing [eprints@whiterose.ac.uk](mailto:eprints@whiterose.ac.uk) including the URL of the record and the reason for the withdrawal request.



[eprints@whiterose.ac.uk](mailto:eprints@whiterose.ac.uk)  
<https://eprints.whiterose.ac.uk/>

# Self-Learning MTPA Control of Interior Permanent Magnet Synchronous Machine Drives Based on Virtual Signal Injection

Tianfu Sun, Student member, IEEE, Jiabin Wang, Senior Member, IEEE, Mikail Koc, Student member, IEEE, Xiao Chen, Student member, IEEE

**Abstract**—This paper describes a simple but effective novel self-learning maximum torque per ampere (MTPA) control scheme for interior permanent magnet synchronous machine (IPMSM) drives to achieve fast dynamic response in tracking the MTPA points without accurate prior knowledge of machine parameters. The proposed self-learning control scheme (SLC) generates the optimal d-axis current command for MTPA operation after training. Virtual signal injection control (VSIC), which has been recently developed as a novel parameter-independent MTPA points tracking scheme, is utilized to train the SLC and compensate the error of the SLC during its operation. In this way, the proposed SLC can achieve the MTPA operation accurately with fast response and the on-line training of the SLC will not affect MTPA operation of IPMSM drives. The proposed control scheme is verified by simulations and experiments under various operation conditions on a prototype IPMSM drive system.

**Index Terms**—Maximum torque per ampere control (MTPA), Permanent magnet synchronous machine (IPMSM), Self-learning control (SLC), Signal injection, Signal processing, Torque control, Virtual signal injection (VSIC)

## I. INTRODUCTION

Due to the high efficiency, high power/torque density, high reliability and good field-weakening performance [1]-[4], the interior permanent magnet synchronous machine (IPMSM) plays an important role in industrial applications especially for electric vehicle traction. In order to control the IPMSM operating at the optimal efficiency points, the maximum torque per ampere (MTPA) control is proposed in [5]-[9]. However, the machine parameters of IPMSMs are highly non-linear due to magnetic saturation, cross-coupling effects, and parameter dependency on temperature [10]-[12]. Parameter variations due to operating conditions and temperature cause great challenges to detect the accurate MTPA point of IPMSM drives.

In order to facilitate accurate MTPA operations of IPMSM drives, look-up tables (LUTs) [12]-[16] and pre-defined MTPA curves are employed by [1], [17] to generate d- and q-axis current reference for MTPA operation. However, the accuracy of look-up tables and pre-defined MTPA curves might greatly be affected by manufacture tolerance, material property varia-

tions and temperature variations. Moreover, generations of the look-up tables and pre-defined MTPA curves not only need expert knowledge and skill, but also are time consuming.

To improve MTPA control accuracy, control schemes for MTPA operation employing on-line parameter estimations are proposed in [18] and [19]. However, the performances of these control schemes are affected by estimation errors and uncertainty in the model structure in which slotting effect and high order magneto-motive force harmonics are often neglected.

Therefore, parameter independent MTPA control technique such as search algorithms [20]-[22] and signal injection control schemes [23]-[28] as well as virtual signal injection control (VSIC) [29], [30] are proposed as an alternative solution. These control schemes are not affected by parameter uncertainty and lead to relatively accurate MTPA operations. However, they suffer from a slow dynamic response as it takes time for the search based schemes to converge to MTPA operating points.

In [31], fuzzy logic is utilized to increase the converging rate of the search algorithm. The output of the fuzzy logic controller in steady state is the change in reference d-axis current and the inputs are the change in power loss and the output of the fuzzy logic controller in the previous step. Although the fuzzy logic controller can increase converge rate, the control scheme is sensitive to current and voltage harmonics and causes torque ripple as a result of d-axis current perturbation.

Another potential solution for improving the convergent rate is to equip these controllers with self-learning. Artificial intelligence based on neural network and fuzzy logic may serve this purpose. However, neural network or fuzzy logic based control schemes in literature [32]-[40] are primarily concerned with speed or position tracking rather than MTPA operations.

One the other hand, if MTPA points can be tracked by parameter independent MPTA control schemes accurately, the tracked MTPA points can be utilized to improve the accuracy and dynamic response of the optimal reference d-axis current generation through on-line training [41]. However, study of seamless integration of on-line training with signal injection based control for MTPA operations have not been reported to date.

In this paper, a novel curve fitting based, on-line training self-learning control scheme is proposed. The training is based on the virtual signal injection control given in [29] as it tracks the MTPA points with high precision and robust to voltage and current harmonics. The VSIC is utilized to track the optimal d-axis current reference for MTPA operation and the proposed

T. Sun, J. Wang, M. Koc and X. Chen are with the Department of Electronic and Electrical Engineering, The University of Sheffield, Mappin Street, Sheffield S1 3JD, United Kingdom (e-mail: tianfu.sun@foxmail.com, j.b.wang@sheffield.ac.uk, mikaalkoc@gmail.com, xiao.chen@sheffield.ac.uk).

SLC scheme is trained on-line by the tracked optimal d-axis current reference. After a period of on-line training, the SLC generates the optimal d-axis current reference for MTPA operation with fast response. In this way, the proposed control scheme not only retains the advantages of virtual signal injection control, such as parameter independence, high accuracy in tracking the MTPA points, and robust to voltage and current harmonics but also has a fast dynamic response. Further the on-line training of the SLC does not affect the MTPA operation of the IPMSM drive.

## II. SELF-LEARNING CONTROL SCHEME FOR MTPA OPERATION

### A. MTPA Point Detection

VSIC based MTPA point tracking control scheme is described in detail in [29]. A high frequency sinusoidal signal  $\Delta\beta$  is injected into machine current angle  $\beta$  with respect to the q-axis:

$$i_d^h = -I_a \sin(\beta + \Delta\beta) \quad (1)$$

$$i_q^h = I_a \cos(\beta + \Delta\beta) \quad (2)$$

where  $I_a$  is measured current amplitude. Since the iron loss influence on MTPA operation is negligible [42], the mechanical power  $P_m$  can be expressed as follows:

$$P_m = \frac{3}{2} [(v_d - Ri_d)i_d + (v_q - Ri_q)i_q] \quad (3)$$

$$P_m = \frac{3}{2} \left[ (v_q - Ri_q) + \frac{(v_d - Ri_d)}{i_q} i_d \right] i_q \quad (4)$$

where  $v_d, v_q$  and  $i_d, i_q$  are d/q-axis reference voltages and d/q-axis measured currents respectively.  $\omega_m$  is the rotor speed, and  $R$  is the phase resistance.

Substitute (1) and (2) into (4), the electromagnetic torque associated with high frequency signal injection can be expressed in (5):

$$T_e^h = \frac{P_m}{\omega_m} = \frac{3}{2} \left[ \frac{(v_q - Ri_q)}{\omega_m} + \frac{(v_d - Ri_d)}{i_q \omega_m} i_d^h \right] i_q^h \quad (5)$$

It has been shown in [26] that if  $T_e^h$  from (5) is processed by the signal processing block shown in Fig.1, the output of the signal processing,  $S$ , will be proportional to  $\partial T_e / \partial \beta$  [29].  $S$  can be defined as a MTPA quality indicator.

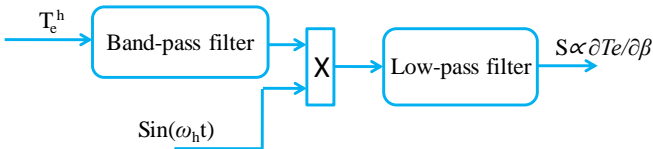


Fig. 1. Signal processing block.

If the MTPA quality indicator  $S$  is fed into an integral regulator with a negative gain, the d-axis current reference can be generated and is adjusted by the VSIC scheme until  $\partial T_e / \partial \beta = 0$  when the MTPA point is reached. It should be noted that (5) which is employed to generate the signal proportional to  $\partial T_e / \partial \beta$  is independent of the motor parameters except the phase resistance. However, since the voltage drop on the re-

sistance is very small, its nominal value at the rated operating temperature will be sufficient to ensure good accuracy.

The MTPA quality indicator  $S$  can also be utilized to identify the d-axis current reference of MTPA operation for a given torque command. The corresponding d-axis current reference and torque reference will be recorded as a tracked MTPA point of the MTPA trajectory shown in Fig. 2.

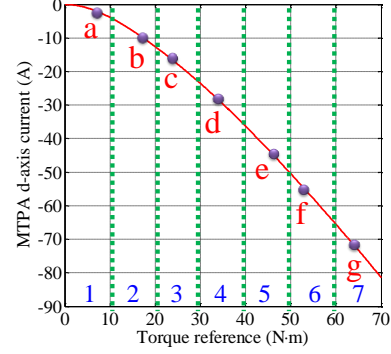


Fig. 2. d-axis current vs. torque for MTPA operation.

It should be noted that MTPA operation is only valid in steady state sense. Thus, the  $S$  signal is masked during d- and q-axis current transients for a small period of 3 times of the current loop time constant.

### B. Principle of Proposed Self-learning Control Scheme

Fig. 2 shows the relationship between reference torque and corresponding optimal d-axis current for MTPA operation. For a given reference torque there is a unique optimal d-axis current for MTPA operation. If a sufficient number of MTPA points on the curve, a to g in Fig. 2, are known, other points on the curve can be approximated by interpolations among these known points. The proposed self-learning control scheme is based on this idea.

As shown in Fig. 2, in order to have an even distribution of recorded MTPA points, the applicable reference torque range of a machine is divided into  $n$  sections and each section records one tracked MTPA point. By way of example, seven sections are shown in Fig. 2. The references torque and their corresponding d-axis currents of tracked MTPA points are recorded as column vectors  $\mathbf{T}_{MTPA}$  and  $\mathbf{i}_{dMTPA}$ . If a new MTPA point is tracked in section  $m$ , the  $m^{\text{th}}$  element of  $\mathbf{T}_{MTPA}$  and  $\mathbf{i}_{dMTPA}$  will be replaced by the corresponding value of the new MTPA point. This process repeats during the SLC operation.

Since MTPA points on the curve can be tracked by VSIC accurately, the training process is performed under VSIC operation. The schematic of the proposed self-learning control scheme is shown in Fig. 3.

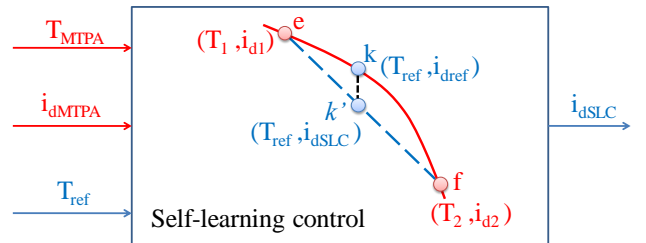


Fig. 3. Schematic of the proposed self-learning control scheme.

Each newly tracked MTPA d-axis current ( $i_{dMTPA}$ ) which is tracked by VSIC and the corresponding torque reference ( $T_{MTPA}$ ) are recorded in the column vectors  $\mathbf{i}_{dMTPA}$  and  $\mathbf{T}_{MTPA}$ , respectively. The two vectors which form the MTPA curve are updated continuously by tracked MTPA points obtained from the VSIC. The recorded data can be used to generate d-axis current reference instantly. For a given torque demand  $T_{ref}$ , the corresponding d-axis current at the MTPA point k in Fig. 3 can be approximated by k' through linear interpolation between the two adjacent MTPA points recorded in  $\mathbf{T}_{MTPA}$  and  $\mathbf{i}_{dMTPA}$ , i.e., the point e and f in Fig. 3, according to (6).

$$i_{dSLC} = \frac{T_{ref} - T_2}{T_1 - T_2} (i_{d1} - i_{d2}) + i_{d2} \quad (6)$$

where  $T_1$  and  $T_2$  are the torque references of e and f, respectively, and  $i_{d1}$  and  $i_{d2}$  are the d-axis currents of e and f.  $i_{dSLC}$  is the output of the self-learning control.

Once the control scheme is trained, the output of SLC ( $i_{dSLC}$ ) should approximate the optimal d-axis current of MTPA operation. If the number of sections is sufficient, the error between the MTPA d-axis current and the SLC output will be very small. The final d-axis current reference will be a combination of  $i_{dSLC}$  and an error compensation component generated from VSIC.

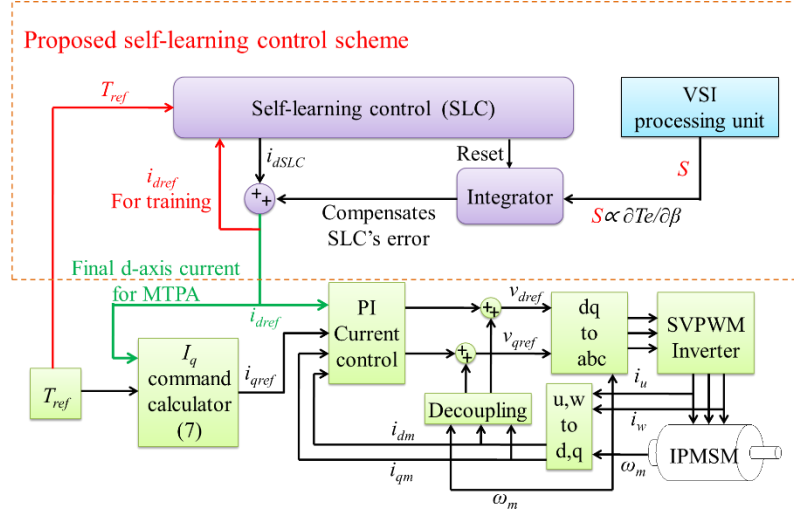


Fig. 4. Schematic of proposed self-learning MTPA control for IPMSM drives.

### C. Description and Features of the Proposed Scheme

The schematic of the proposed self-learning control scheme for MTPA operation is shown in Fig. 4. It consists of conventional PI current control loops for tracking the reference d-axis and q-axis currents, a virtual signal injection (VSI) processing unit, and a self-learning controller. The output of the VSI processing unit is fed to an integrator. The d-axis current reference is the sum of the SLC output and the integrated output.

Before training, the  $\mathbf{T}_{MTPA}$  and  $\mathbf{i}_{dMTPA}$  are zero vectors initially, or data associated with the MTPA curve generated off-line using nominal motor parameters may be stored. If a torque demand,  $T_{ref}$  in Fig. 4, is larger than the maximum value in vector  $\mathbf{T}_{MTPA}$ , the output,  $i_{dSLC}$ , of the self-learning control will equal to the element in vector  $\mathbf{i}_{dMTPA}$  which corresponds to the maximum torque reference in  $\mathbf{T}_{MTPA}$ . If  $T_{ref}$  is located between two elements of  $\mathbf{T}_{MTPA}$ , as shown in Fig. 3, the  $i_{dSLC}$  can be obtained through linear interpolation of the two recorded MTPA points according to (6). Before the SLC controller is fully trained, its output may deviate from the MTPA point by a large margin. However, any error will be adjusted by the integrator output until the output,  $S$ , of VSI processing block approximate to zero, i.e., the MTPA operation is realized [29].

Since the integrator in Fig. 4 will accumulate value, in order to increase d-axis current response, at each time when the absolute value of reference torque step is larger than a pre-defined threshold,  $\epsilon$ , the integrator will be reset. Meanwhile the  $i_{dSLC}$

will be updated according to the new reference torque based on the data recorded in  $\mathbf{T}_{MTPA}$  and  $\mathbf{i}_{dMTPA}$  when the integrator is reset. For the condition that the torque step is smaller than the threshold, because the corresponding change in d-axis current should be small too, the  $i_{dSLC}$  will not update and the small error will be compensated by the virtual signal injection in short time. The  $\mathbf{T}_{MTPA}$  and  $\mathbf{i}_{dMTPA}$  will be updated continuously by the reference torque and resultant d-axis current. The exact value of the predefined threshold  $\epsilon$  is not important, as it only affects slightly the MTPA tracking response.

When a torque step is larger than the threshold,  $S$  signal will be masked for a small period of time. After this period, the virtual signal injection will drive the resultant d-axis current toward the MTPA point and the  $\mathbf{T}_{MTPA}$  and  $\mathbf{i}_{dMTPA}$  will be updated continuously by the reference torque and the resultant d-axis current. Since the virtual signal injection adjusts the d-axis current towards the MTPA point, the resultant d-axis current can be considered as the  $i_{dMTPA}$  in Section II Part B and the newly recorded d-axis current in  $\mathbf{i}_{dMTPA}$  should be very closer to the actual MTPA point than the previously recorded in  $\mathbf{i}_{dMTPA}$ . Therefore, the accuracy of SLC output will continuously be improved. Moreover, a more accurate SLC output will also accelerated the convergent rate of the d-axis current to the actual MTPA point. Therefore, although the MTPA d-axis currents recorded in  $\mathbf{i}_{dMTPA}$  may initially have large error, they will eventually approach the ideal MTPA d-axis currents. Consequently, the proposed SLC can be trained on-line, and the training of the SLC will not affect the MTPA operation.

The q-axis reference current in Fig.4 is generated from (7) base on the torque reference and d-axis current reference.

$$i_{qref} = \frac{T_{ref}}{\frac{3}{2}p[\Psi_m + (L_d - L_q)i_{dref}]} \quad (7)$$

where  $L_d$ ,  $L_q$  and  $\Psi_m$  in are d- and q-axis inductances and permanent magnet flux linkage, respectively. The machine parameters employed in (7) can either be the nominal machine parameters or obtained from look-up tables as functions of d- and q-axis currents. It should be noted that if the parameters in (7) are inaccurate, the q-axis current will not yield the exact torque reference, and there will be torque control error. However, since the signal  $T_e^h$  in (5) which corrects the d-axis current is independent from these parameters, the resultant d-axis current still ensures that the motor operates on the MTPA points for the actual torque. The gap in the reference and actual torque can be corrected by the speed feedback loop in a speed servo drive. For EV tractions however, the feedback correction will be performed by a human driver. Of course, if high fidelity model parameters are stored in a look-up table, the torque control accuracy can be improved.

### III. SIMULATION OF THE PROPOSED CONTROL SCHEME

To verify the performance of the proposed self-learning control scheme, simulations were performed employing a high fidelity non-linear IPMSM machine model which represents the real electromagnetic behaviors of the IPMSM. The high fidelity model is flux linkage-based and captures all non-linear effects and high order space harmonics as described in [43]. The machine specifications are listed in Table I. The motor was controlled in torque control mode in simulations. The applicable torque reference range of a machine is divided into 35 sections. The q-axis reference current was calculated based on (7) and the machine parameters in (7) were obtained from predefined look-up tables as functions of d- and q- axis currents.

TABLE I  
IPMSM Parameters

Number of pole-pairs	3
Phase resistance	51.2 mΩ
Continuous/Maximum current	58.5/118 A
Peak power below base speed	10 kW
DC link voltage	120 V
Based/maximum speed	1350/4500 rpm
Continuous/peak torque	35.5/70 N·m
Peak power at maximum speed	7 kW

Fig. 5 shows the variations of the resultant torque and d-axis current reference together with the SLC output when the torque varied between 9N·m and 68N·m in steps periodically.

When  $t < 35s$ , the SLC output was equal to the d-axis current reference recorded in  $i_{dMTPA}$  which is corresponding to the maximum torque reference in  $T_{MTPA}$ . The error between MTPA d-axis current for the torque reference  $T_{ref}$  and SLC output was compensated by the VSIC, albeit its response was slow. However, when the proposed self-learning control scheme was trained, i.e., when  $t > 35s$ , the output of SLC approximated the MTPA d-axis current and the approximation error was small. This error was still compensated by the VSIC. The speed of tracking response of the proposed control has been significantly

increased.

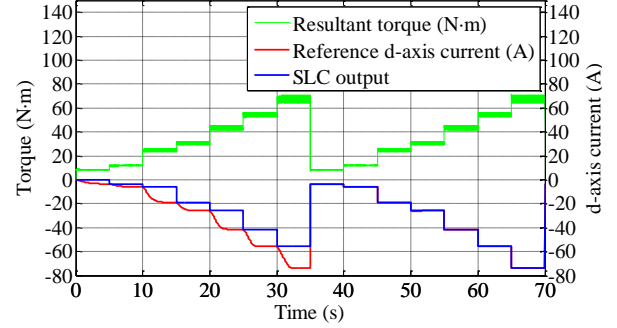


Fig. 5. Variations of resultant torque and d-axis reference current from SLC.

The simulation results of the MTPA quality indicator,  $S$ , and d-axis current reference generated from the proposed self-learning control scheme under the same operating conditions as Fig. 5 are shown in Fig. 6. It can be seen from Fig.6, before the proposed self-learning control scheme was trained, i.e.,  $t < 35s$ , at each torque reference step, the output of the signal processing block is initially large and then converged to zero gradually. This is because the large error of untrained SLC output and the tracking of the MTPA d-axis current references by the virtual signal injection has relatively slow converging rate. After the proposed self-learning control scheme has been trained, the output of the signal processing block becomes small and the d-axis reference current responds quickly to the torque change. Moreover,  $S$  always converges to zero, which implies that the d-axis current converges to the MTPA point and the training of the proposed self-learning control scheme base on the virtual signal injection control is accurate.

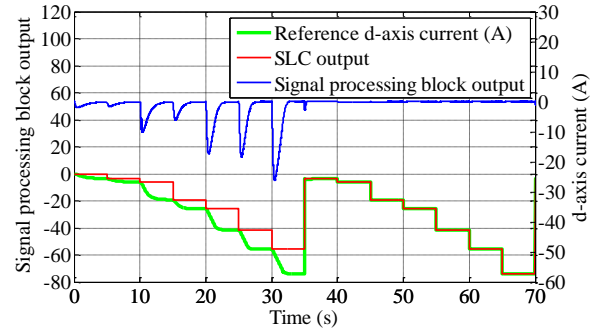


Fig. 6. The simulation result of  $S$  and d-axis current reference generation.

The resultant torque and the output of integrator in Fig. 4 is shown in Fig. 7. The threshold to reset the integrator in this paper is set to  $2N \cdot m$ . As shown in Fig. 7, before the proposed control scheme is trained, i.e.,  $t < 35s$ , the values accumulated in the integrator are large and the integrator will be reset in every torque step. However, after the proposed control scheme is trained, the optimal d-axis current can be directly generated from the SLC and the output of integrator is close to zero. Therefore whether it is reset or not will no longer has much effect.

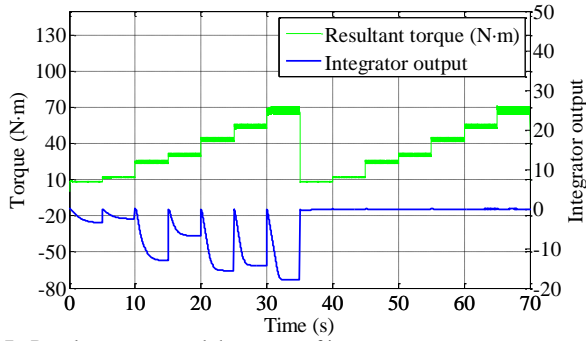


Fig. 7. Resultant torque and the output of integrator.

At  $t=70$ s, the permanent magnet (PM) flux linkage in the machine model was reduced to 80 percent of its original value while the parameters in (7) used to compute the q-axis current reference were not changed. This may represent the combined effect of temperature increase and partial demagnetization of the machine. The change in the PM flux linkage caused the new MTPA point to deviate from the original MTPA point and the VSIC compensated the deviation. Meanwhile the  $T_{MTPA}$  and  $i_{dMTPA}$  are updated according to newly identified MTPA points.

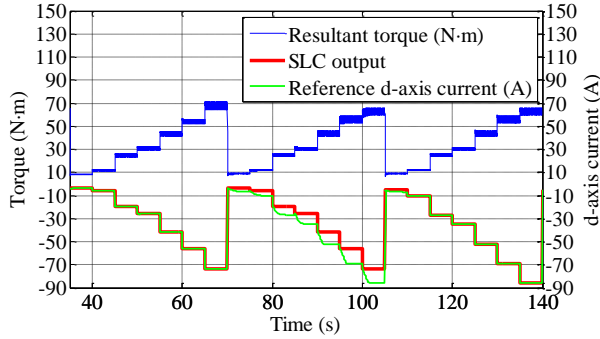


Fig. 8. SLC behavior after machine parameter changes.

It can be seen from Fig. 8 that in the first cycle after the parameter changed (from  $t=70$ s to  $t=105$ s), the d-axis current reference was obtained from the sum of SLC output and VSIC with relatively slow response. During this period, the proposed SLC was trained by the newly tracked MTPA d-axis current references. In the second cycle after the machine parameter changed ( $t>105$ s), the proposed SLC has adapted itself to the new machine parameters and the output of the SLC reached the MTPA d-axis current reference tracked by VSIC of the new operation condition with fast response. And the training of the SLC did not affect MTPA operation of the IPMSM drive, albeit the torque control error increased.

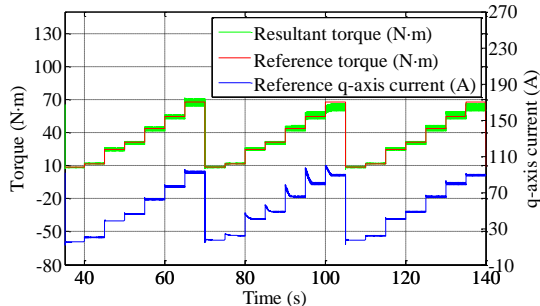


Fig. 9. Simulation results of torque reference, resultant torque as well as q-axis current.

The simulated torque and q-axis current responses under the same operating conditions as Fig. 8 are shown in Fig. 9. Due to the change in the PM flux linkage, the torque error became significant. If continuous operation is thermally sustainable, the error can be compensated by the speed loop in a speed controlled drive system. While in EV traction, the loop is closed by the vehicle driver.

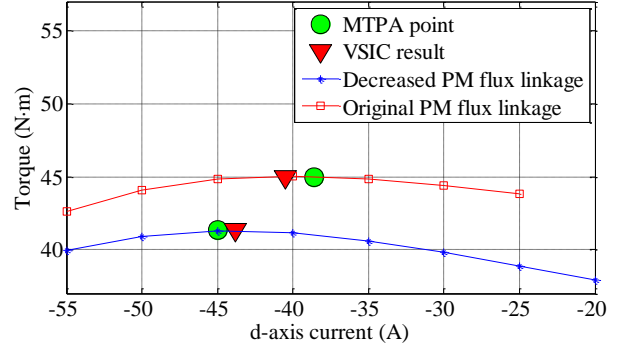


Fig. 10. Constant current amplitude curves and VSIC tracking performance with inaccurate q-axis current.

Fig. 10 illustrates the constant current amplitude curves for different PM flux linkages and compares the simulation results obtained from the original PM flux linkage and reduced PM flux linkage for the reference torque of  $45\text{N}\cdot\text{m}$ . It can be seen from Fig. 10, although the machine parameter in (7) was not accurate and the resultant torque was not equal to the torque reference, the VSIC can still track the MTPA point accurately.

Fig. 11 shows the simulation results when the reference torque step is smaller than the threshold. When  $t<35$ s, the proposed control scheme is not trained while the reference torque slowly increased with a  $2\text{N}\cdot\text{m}/\text{s}$  gradient. Under this condition, the integrator in Fig. 4 will not be reset and  $i_{dSLC}$  will not be updated. The d-axis reference is generated from the integrator based on the virtual signal injection and the proposed control scheme is still trained under this condition. When  $t>35$ s, the optimal d-axis current is generated from the SLC directly with fast response.

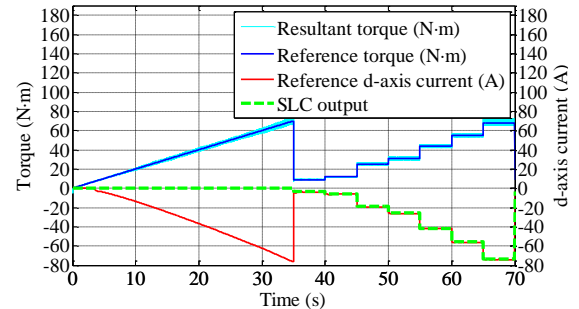


Fig. 11. Training performance when reference torque changes slowly.

Simulations were also performed for the operating condition when the reference torque changes rapidly. As shown in Fig. 12, the reference torque changes in steps between  $20\text{N}\cdot\text{m}$  and  $40\text{N}\cdot\text{m}$  in every 2s. Before the proposed control scheme is fully trained, i.e.,  $t<6$ s, the virtual signal injection adjusts the d-axis current toward the MTPA d-axis current and the corresponding reference torque and d-axis current is recorded in  $T_{MTPA}$  and  $i_{dMTPA}$ . At each torque step, the integrator is reset meanwhile the SLC output is updated based on the data recorded in  $T_{MTPA}$

and  $i_{dMTPA}$ , simultaneously. As it can be seen in Fig. 12, the accuracy of the SLC output continuously improves and eventually equal to the optimal values. The speed of tracking response of the proposed control has been significantly increased after the training.

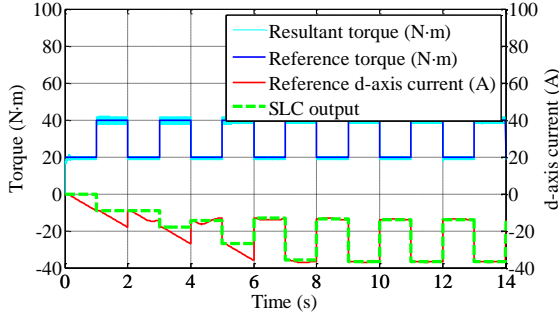


Fig. 12. Training performance when reference torque changes rapidly.

#### IV. EXPERIMENT RESULTS

To verify the proposed self-learning control scheme, experiments were performed on a 10kW IPMSM drive whose specification is given in Table I. The test rig for the experiments is shown in Fig. 13. The motor was control in torque control mode and loaded by a dynamometer. The resultant torque was measured by a high precision torque transducer. The frequency and amplitude of the virtual signal injection was 1000Hz and 0.001rad, respectively. And a 4<sup>th</sup> order band-pass filter with a band width of 1Hz at the center frequency of the virtually injected signal was adopted by the VSI. The applicable torque reference range of the machine was divided into 35 sections as those in the simulations. The threshold to reset the integrator in this paper is set to  $2N \cdot m$ .

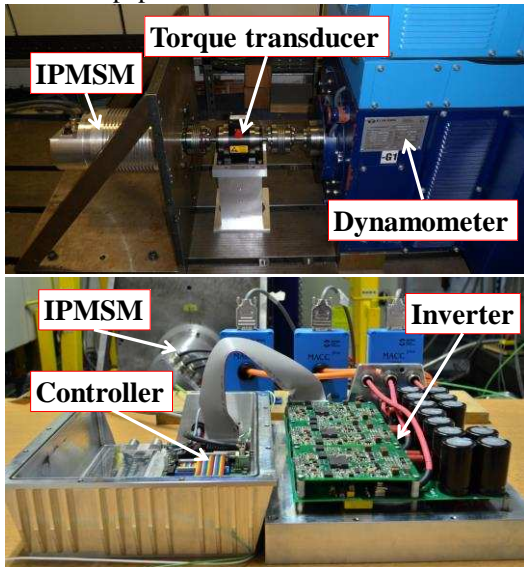


Fig. 13. Experimental test-rig.

##### A. MTPA Points Tracking Performance

The MTPA points tracking performances in steady state are illustrated in Fig. 14. As shown in Fig. 14, the payload torque was increased from  $10N \cdot m$  to  $45N \cdot m$  in a step of  $5N \cdot m$  at 1000r/min. To determine MTPA points experimentally, torque variation with current angle when the current amplitude was

kept constant was measured for each payload torque. The actual MTPA points are obtained through curve fitting of the measured torque data and they are represented in Fig. 14 by squares. Meanwhile, the proposed control was implemented by initial disable the SLC unit. Hence, the d-axis current references were generated by the virtual signal injection control scheme and the q-axis current were generated according to (7). The VSIC based MTPA points tracking results are represented by circles.

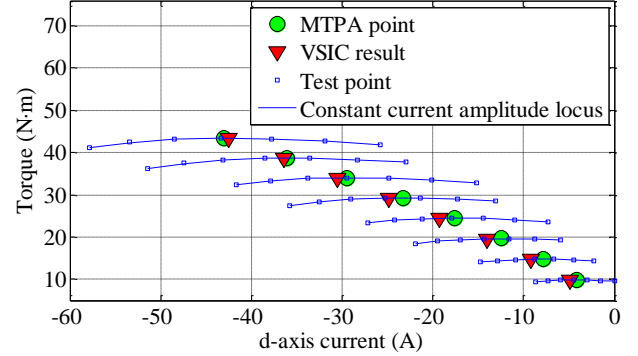


Fig. 14. Experimental result of VSIC's MTPA tracking performance

Table II compares the resultant torques of the VSIC and the measured torques at the MTPA points. It can be seen from Fig. 14 and Table II that the VSIC can always track the MTPA points with high accuracy and the torque error between the measured MTPA points and VSIC is less than 0.2%. It is also evident that the measured output torque under the VSIC is slightly lower than the torque reference. This is because the parameters in (7) are not accurate and presence of friction torque in the real machine.

TABLE II

Comparison between Resultant Torque of VSIC and Torque of MTPA Points at 1000r/min

Torque reference	Current amplitude	Torque generated by VSIC	MTPA torque	Torque error
10N·m	17.26 A	9.85N·m	9.86N·m	0.10%
15N·m	25.67 A	14.74N·m	14.77N·m	0.20%
20N·m	34.00 A	19.60N·m	19.64N·m	0.20%
25N·m	42.28 A	24.43N·m	24.47N·m	0.16%
30N·m	50.55 A	29.25N·m	29.27N·m	0.07%
35N·m	58.87 A	34.02N·m	34.04N·m	0.06%
40N·m	67.10 A	38.72N·m	38.72N·m	0.00%
45N·m	75.47 A	43.42N·m	43.42N·m	0.00%

##### B. Performance of Proposed Control Scheme during Payload Torque Changes.

To validate the performance of the proposed self-learning control scheme during payload torque changes, the proposed control scheme was firstly tested with torque reference variations from  $0N \cdot m$  to  $35N \cdot m$  in a step of  $5N \cdot m$  at 1000r/min. The proposed scheme was trained during this process. Subsequently, the torque reference was decreased from  $35N \cdot m$  to  $0N \cdot m$  in a step of  $5N \cdot m$  and the  $i_{dSLC}$  was generated from the tracked MTPA points which were recorded in  $T_{MTPA}$  and  $i_{dMTPA}$ . Finally, the torque reference was increased from  $3N \cdot m$  to  $28N \cdot m$  in a step of  $5N \cdot m$  at 1000r/min so that the references do not coincide with the training data in order to valid the SLC

performance at the operation conditions which the drive had not experienced previously.

Fig. 15 shows the measured d-axis current together with measured torque and estimated torque when the torque reference is stepped from  $20\text{N}\cdot\text{m}$  to  $35\text{N}\cdot\text{m}$  in steps of  $5\text{N}\cdot\text{m}$  and back to  $20\text{N}\cdot\text{m}$  in the same steps. The estimated torque was based on the high fidelity machine model and measured d- and q-axis currents.

As shown in Fig. 15, when torque reference stepped from  $25\text{N}\cdot\text{m}$  to  $30\text{N}\cdot\text{m}$  during the time  $t < 60\text{s}$ , the SLC had not been trained at  $30\text{N}\cdot\text{m}$  torque reference but had been trained at the  $25\text{N}\cdot\text{m}$ . The output of the SLC was equal to the element in  $\mathbf{i}_{dMTPA}$  which corresponds to the maximum torque reference in  $T_{MTPA}$ , e.g., the MTPA d-axis current of  $25\text{N}\cdot\text{m}$ . The error between the output of SLC and the MTPA d-axis current for  $30\text{N}\cdot\text{m}$  torque reference was compensated by the VSIC albeit the d-axis current responded to the torque step slowly. Similar result can be observed when the torque reference is stepped from  $30\text{N}\cdot\text{m}$  to  $35\text{N}\cdot\text{m}$ .

When the torque reference is stepped from  $35\text{N}\cdot\text{m}$  to  $30\text{N}\cdot\text{m}$ , since the SLC had been trained at  $30\text{N}\cdot\text{m}$  torque reference before, the output of the SLC approximated to the optimal d-axis current for the MTPA operation. As shown in Fig. 15, the speed of tracking response of the proposed control was significantly increased and similar results can be observed when the torque reference is stepped from  $30\text{N}\cdot\text{m}$  to  $25\text{N}\cdot\text{m}$ . The integrator output is shown in Fig. 16 for the purpose of illustration. Once the controller is trained, the d-axis reference current is directly generated from the SLC, and hence the integrator output from the VSIC is closed to zero. It should be noted that the torque ripple in the measured torque is smaller than that in the estimated torque due to the low-pass filter effect in the torque transducer and its signal conditioning system.

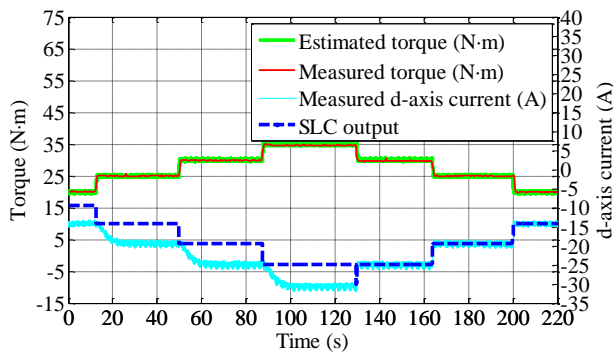


Fig. 15. d-axis current and estimated/measured torque response to torque command step from  $20\text{N}\cdot\text{m}$  to  $35\text{N}\cdot\text{m}$  then step back to  $20\text{N}\cdot\text{m}$ .

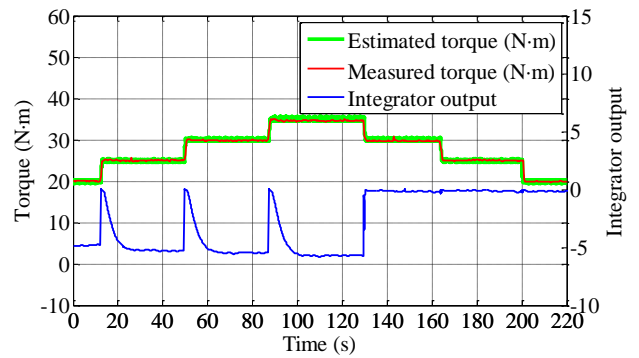


Fig. 16 Integrator output together with the measured and estimated torque responses.

Fig. 17 shows the variations of the measured torque and the measured q-axis current which corresponds to the d-axis current reference variations shown in Fig. 15. Before the SLC was trained, the q-axis current always had large overshoot due to the slow d-axis current response. However, after the SLC was trained, the overshoot was significantly reduced.

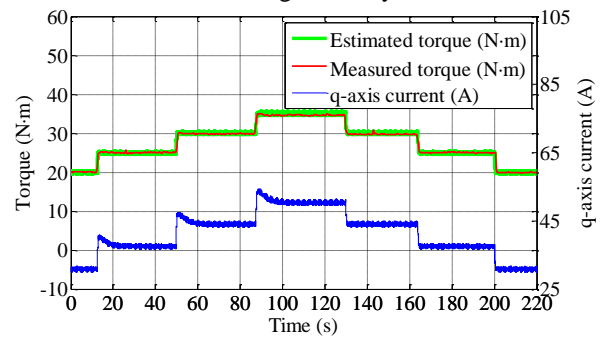


Fig. 17. The estimated/measured torque and the measured q-axis current.

The torque reference was also increased from  $3\text{N}\cdot\text{m}$  to  $28\text{N}\cdot\text{m}$  in a step of  $5\text{N}\cdot\text{m}$  at  $1000\text{r}/\text{min}$  during the tests. Although the SLC was not trained at these torque references, since they were located between trained torque references, the SLC can still generate the d-axis current references for MTPA control accurately.

Fig. 18 illustrates the d-axis current response when the torque reference is stepped from  $8\text{N}\cdot\text{m}$  to  $13\text{N}\cdot\text{m}$  after the SLC has been trained. From Fig. 18, a fast d-axis current response as well as measured torque response can be observed. This illustrates that the proposed SLC can produce the MTPA d-axis current even for the torque reference which it has not experienced before.

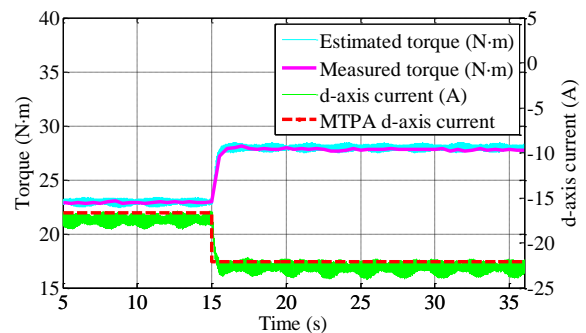


Fig. 18. d-axis current and estimated/measured torque response to torque command step from  $8\text{N}\cdot\text{m}$  to  $13\text{N}\cdot\text{m}$ .

## CONCLUSION

The proposed self-learning control scheme employs curve fitting to establish the relationship between the torque and the d-axis current for MTPA operation. The proposed control scheme is trained from the MTPA points tracked by the virtual signal injection control scheme during drive operation. After the proposed control scheme has been trained, the d-axis current command for MTPA operation is directly generated from the self-learning control scheme for a given torque reference. Meanwhile, the virtual signal injection control scheme can still be utilized to compensate any error between the d-axis current command generated by the SLC and the ideal d-axis current for MTPA operation. The simulation and experiment results show that the proposed SLC scheme can generate accurate d-axis current command to ensure MTPA operation with fast response. The proposed control technique offers accurate MTPA tracking with fast torque response while being independent of machine parameter variations, and hence provides an effective mean for efficient operation of IPMSM drives.

## REFERENCES

- [1] S. Morimoto, Y. Takeda, and T. Hirasu, "Current phase control methods for permanent magnet synchronous motors," *IEEE Trans. Power Electron.*, vol. 5, no. 2, pp. 133–139, Apr. 1990.
- [2] T. Miyajima, H. Fujimoto, and M. Fujitsuna, "A Precise Model-Based Design of Voltage Phase Controller for IPMSM," *IEEE Trans. Power Electron.*, vol. 28, no. 12, pp. 5655–5664, 2013.
- [3] S. Bolognani, S. Calligaro, and R. Petrella, "Adaptive Flux-Weakening Controller for Interior Permanent Magnet Synchronous Motor Drives," *IEEE J. Emerg. Sel. Top. Power Electron.*, vol. 2, no. 2, pp. 236–248, Jun. 2014.
- [4] O. Wallmark, S. Lundberg, and M. Bongiorno, "Input Admittance Expressions for Field-Oriented Controlled Salient PMSM Drives," *IEEE Trans. Power Electron.*, vol. 27, no. 3, pp. 1514–1520, Mar. 2012.
- [5] M. N. Uddin, T. S. Radwan, and M. A. Rahman, "Performance of Interior Permanent Magnet Motor Drive Over Wide Speed Range," *IEEE Trans. Energy Convers.*, vol. 17, no. 1, pp. 79–84, 2002.
- [6] C. T. Pan and S. M. Sue, "A Linear Maximum Torque Per Ampere Control for IPMSM Drives Over Full-Speed Range," *IEEE Trans. Energy Convers.*, vol. 20, no. 2, pp. 359–366, Jun. 2005.
- [7] S. Morimoto, K. Hatanaka, Y. Tong, Y. Takeda, and T. Hirasu, "Servo Drive System and Control Characteristics of Salient Pole Permanent Magnet Synchronous Motor," *IEEE Trans. Industry Appl.*, vol. 29, no. 2, pp. 338–343, 1993.
- [8] T. M. Jahns, G. B. Kliman, and T. W. Neumann, "Interior Permanent-Magnet Synchronous Motors for Adjustable-Speed Drives," *IEEE Trans. Industry Appl.*, vol. IA-22, no. 4, pp. 738–747, Jul. 1986.
- [9] S. Morimoto, M. Sanada, and Y. Takeda, "Wide-speed operation of interior permanent magnet synchronous motors with high-performance current regulator," *IEEE Trans. Industry Appl.*, vol. 30, no. 4, pp. 920–926, 1994.
- [10] K. D. Hoang, J. Wang, M. Cyriacks, A. Melkonyan, and K. Kriegl, "Feed-forward Torque Control of Interior Permanent Magnet Brushless AC Drive for Traction Applications," in *Proc. IEEE Electric Machines & Drives Conf.*, 2013, pp. 152–159.
- [11] B. Štumberger, G. Štumberger, D. Dolinar, A. Hamler, and M. Trlep, "Evaluation of saturation and cross-magnetization effects in interior permanent-magnet synchronous motor," *IEEE Trans. Industry Appl.*, vol. 39, no. 5, pp. 1264–1271, Sep. 2003.
- [12] G. Kang, J. Lim, K. Nam, H.-B. Ihm, and H.-G. Kim, "A MTPA Control Scheme for an IPM Synchronous Motor Considering Magnet Flux Variation Caused by Temperature," in *Proc. IEEE Applied Power Electronics Conf.*, 2004, pp. 1617–1621.
- [13] N. Yang, G. Luo, W. Liu, and K. Wang, "Interior permanent magnet synchronous motor control for electric vehicle using look-up table," in *Proc. IEEE Power Electronics and Motion Control Conf.*, 2012, pp. 1015–1019.
- [14] S. Jung, J. Hong, and K. Nam, "Current Minimizing Torque Control of the IPMSM Using Ferrari's Method," *IEEE Trans. Power Electron.*, vol. 28, no. 12, pp. 5603–5617, 2013.
- [15] Y. S. Kim and S. K. Sul, "Torque Control Strategy of an IPMSM Considering the Flux Variation of the Permanent Magnet," in *Proc. IEEE Industry Applications Conf.*, 2007, pp. 1301–1307.
- [16] A. Consoli, G. Scarcella, G. Scelba, and A. Testa, "Steady-State and Transient Operation of IPMSMs Under Maximum-Torque-per-Ampere Control," *IEEE Trans. Industry Appl.*, vol. 46, no. 1, pp. 121–129, 2010.
- [17] S. Morimoto, K. Hatanaka, Y. Tong, Y. Takeda, and T. Hirasu, "High performance servo drive system of salient pole permanent magnet synchronous motor," in *Proc. IEEE Industry Applications Society Annual Meeting*, 1991, pp. 463–468.
- [18] P. Niazi, H. a. Toliyat, and A. Goodarzi, "Robust maximum torque per ampere (MTPA) control of PM-assisted SynRM for traction applications," *IEEE Trans. Industry Appl.*, vol. 56, no. 4, pp. 1538–1545, 2007.
- [19] Y. A.-R. I. Mohamed and T. K. Lee, "Adaptive Self-Tuning MTPA Vector Controller for IPMSM Drive System," *IEEE Trans. Energy Convers.*, vol. 21, no. 3, pp. 636–644, Sep. 2006.
- [20] R. S. Colby and D. W. Novotny, "An Efficiency-Optimizing Permanent-Magnet Synchronous Motor Drive," *IEEE Trans. Industry Appl.*, vol. 24, no. 3, pp. 462–469, 1988.
- [21] A. Dianov, Y. Kk. Kim, S. J. Lee, and S. T. Lee, "Robust Self-Tuning MTPA Algorithm for IPMSM Drives," in *Proc. IEEE Industrial Electronics Conf.*, 2008, pp. 1355–1360.
- [22] K. W. Lee and S. Bin Lee, "MTPA operating point tracking control scheme for vector controlled PMSM drives," in *IEEE Symposium on Power Electronics Electrical Drives Automation and Motion*, 2010, pp. 24–28.
- [23] S. Bolognani, L. Peretti, and M. Zigliotto, "Online MTPA Control Strategy for DTC Synchronous-Reluctance-Motor Drives," *IEEE Trans. Power Electron.*, vol. 26, no. 1, pp. 20–28, Jan. 2011.
- [24] S. Bolognani, R. Petrella, A. Prearo, and L. Sgarbossa, "Automatic Tracking of MTPA Trajectory in IPM Motor Drives Based on AC Current Injection," *IEEE Trans. Industry Appl.*, vol. 47, no. 1, pp. 105–114, Jan. 2011.
- [25] R. Antonello, M. Carraro, and M. Zigliotto, "Towards the automatic tuning of MTPA algorithms for IPM motor drives," in *Proc. IEEE Electrical Machines Conf.*, 2012, pp. 1121–1127.
- [26] R. Antonello, M. Carraro, and M. Zigliotto, "Theory and implementation of a MTPA tracking controller for anisotropic PM motor drives," in *Proc. IEEE Industrial Electronics Society - 38th Annual Conf.*, 2012, pp. 2061–2066.
- [27] R. Antonello, M. Carraro, and M. Zigliotto, "Maximum-Torque-Per-Ampere Operation of Anisotropic Synchronous Permanent-Magnet Motors Based on Extremum Seeking Control," *IEEE Trans. Industrial Electron.*, vol. 61, no. 9, pp. 5086–5093, Sep. 2014.
- [28] S. Kim, Y. D. Yoon, S. K. Sul, and K. Ide, "Maximum Torque per Ampere (MTPA) Control of an IPM Machine Based on Signal Injection Considering Inductance Saturation," *IEEE Trans. Power Electron.*, vol. 28, no. 1, pp. 488–497, 2013.
- [29] T. Sun, J. Wang, and X. Chen, "Maximum Torque per Ampere (MTPA) Control for Interior Permanent Magnet Synchronous Machine Drives Based on Virtual Signal Injection," *IEEE Trans. Power Electron.*, vol. 30, no. 9, pp. 5036–5045, 2015.
- [30] T. Sun and J. Wang, "Extension of Virtual Signal Injection Based MTPA Control for Interior Permanent Magnet Synchronous Machine Drives into Field Weakening Region," *IEEE Trans. Industrial Electron.*, vol. 62, no. 11, pp. 6809–6817, 2015.
- [31] M. N. Uddin and J. Khastoo, "Fuzzy logic-based efficiency optimization and high dynamic performance of IPMSM drive system in both transient and steady-state conditions," *IEEE Trans. Industry Appl.*, vol. 50, no. 6, pp. 4251–4259, 2014.
- [32] Y. Yi, D. M. Vilathgamuwa, and M. A. Rahman, "Implementation of an artificial-neural-network-based real-time adaptive controller for an interior permanent-magnet motor drive," *IEEE Trans. Industry Appl.*, vol. 39, no. 1, pp. 96–104, 2003.
- [33] C. B. Butt and M. Azizur Rahman, "Untrained artificial neuron-based speed control of interior permanent-magnet motor drives over extended operating speed range," *IEEE Trans. Industry Appl.*, vol. 49, no. 3, pp. 1146–1153, 2013.
- [34] M. N. Uddin, M. a. Abido, and M. a. Rahman, "Development and implementation of a hybrid intelligent controller for interior permanent-magnet synchronous motor drives," *IEEE Trans. Industry Appl.*, vol. 40, no. 1, pp. 68–76, 2004.

- [35] A. Rubaai and P. Young, "Hardware/software implementation of fuzzy neural network self-learning control methods for brushless DC motor drives," *IEEE Trans, Industry Appl.*, vol. in press, 2015.
- [36] A. Rubaai and P. Young, "EKF-based PI/PD-like fuzzy-neural-network controller for brushless drives," *IEEE Trans, Industry Appl.*, vol. 47, no. 6, pp. 2391–2401, 2011.
- [37] S. Kang, J. Ko, J. Choi, J. Baek, and D. Chung, "Maximum Torque Control of IPMSM Drive with Multi-MFC," in *Proc. Control Automation and Systems (ICCAS)*, 2010 International Conference on, 2010, pp. 1242–1247.
- [38] L. Guo and L. Parsa, "Model Reference Adaptive Control of Five-Phase IPM Motors Based on Neural Network," *IEEE Trans, Industrial Electron.*, vol. 59, no. 3, pp. 1500–1508, 2012.
- [39] M. S. Hossain and M. J. Hossain, "Performance Analysis of a Novel Fuzzy Logic and MTPA Based Speed Control for IPMSM Drive with variable d- and q-axis Inductances," in *Proc. Computers and Information Technology, International Conference on*, 2009, no. Iccit, pp. 21–23.
- [40] C. B. Butt, M. A. Hoque, and M. A. Rahman, "Simplified Fuzzy-Logic-Based MTPA Speed Control of IPMSM Drive," *IEEE Trans, Industry Appl.*, vol. 40, no. 6, pp. 1529–1535, 2004.
- [41] T. Sun, J. Wang, M. Koc, and X. Chen, "Self-Learning MTPA Control of Interior Permanent Magnet Synchronous Machine Drives Based on Virtual Signal Injection," in *Proc. IEEE Int. Electr. Mach. Drives Conf. (IEMDC)*, 2015.
- [42] A. Ruf, A. Thul, S. Steentjes, and K. Hameyer, "Loss minimizing control strategy for electrical machines considering iron loss distribution," in *Proc. IEEE Int. Electr. Mach. Drives Conf. (IEMDC)*, 2015.
- [43] X. Chen, J. Wang, B. Sen, P. Lazari, and T. Sun, "A High-Fidelity, Computationally Efficient Model for Interior Permanent Magnet Machines Considering the Magnetic Saturation, Spatial Harmonics and Iron Loss Effect," *IEEE Trans, Industrial Electron.*, vol. 62, no. 7, pp. 4044–4055, 2015.



**Tianfu Sun** (S'15) was born in China. He received B.Eng. degree in mechanical engineering and M.Sc. degree in civil engineering from Dalian University of Technology, Dalian, China, in 2009 and 2012, respectively.

He is currently pursuing the Ph.D. degree in electronic and electrical engineering at The University of Sheffield, U.K. His current research interests include electric/hybrid

vehicle drives, power-electronic control of electric machines, sensorless drives and artificial intelligence.



**Jiabin Wang** (SM'03) received the B.Eng. and M.Eng. degrees from Jiangsu University of Science and Technology, Zhenjiang, China, in 1982 and 1986, respectively, and the Ph.D. degree from the University of East London, London, U.K., in 1996, all in electrical and electronic engineering.

Currently, he is a Professor in Electrical Engineering at the University of Sheffield, Sheffield, U.K. From 1986 to 1991, he was

with the Department of Electrical Engineering at Jiangsu University of Science and Technology, where he was appointed a Lecturer in 1987 and an Associated Professor in 1990. He was a Postdoctoral Research Associate at the University of Sheffield, Sheffield, U.K., from 1996 to 1997, and a Senior Lecturer at the University of East London from 1998 to 2001. His research interests range from motion control and electromechanical energy conversion to electric drives for applications in automotive, renewable energy, household appliances and aerospace sectors.

He is a fellow of the IET and a senior member of IEEE.



**Mikail Koc** (S'15) was born in Turkey. He received the BSc degree from ESOGU University, Eskisehir, Turkey, in 2009 and the MSc degree from Nottingham University, UK, in 2012 both in electrical and electronic engineering. He is currently pursuing the PhD degree in electronic and electrical engineering at the University of Sheffield, UK. His research interests include efficiency optimised control of motors for

electric vehicle traction.



**Xiao Chen** (S'13) born in Taian, China, in 1988, received B.Eng. degree in electrical engineering from Harbin Institute of Technology at Weihai, Weihai, China, in 2009, and received M.Eng. degree in electrical engineering from Harbin Institute of Technology, Harbin, China, in 2011, respectively. Now he is working towards the Ph.D degree in the Dept. of Electronic and Electrical Engineering, The University of Sheffield, UK. His current research interests include the modeling, design and analysis of permanent-magnet synchronous machines for traction applications.